10th International Workshop on Ship and Marine Hydrodynamics
Keelung, Taiwan, November 5-8, 2017

Fully coupled effects on waves and barge with single sloshing tank by CFD methods

Yuan Zhuang, Decheng Wan*
Collaborative Innovation Center for Advanced Ship and Deep-Sea Exploration, State Key Laboratory of Ocean Engineering, School of Naval Architecture, Ocean and Civil Engineering, Shanghai Jiao Tong University, Shanghai, China

*Corresponding author: dcwan@sjtu.edu.cn

ABSTRACT

With the demands for natural gas and sources in deep sea, the ship with partially filled tanks becomes more and more popular. The ship motion is an external excitation for sloshing tank, and sloshing tank would influence ship motion in return. In this paper, fully coupled effects on ship motion and a single sloshing tank is discussed using our in-house CFD solver naoe-FOAM-SJTU, which is developed and based on open source toolbox OpenFOAM. The coupling effects are observed between waves and the box with two tanks, and only one tank is partially filled. Only sway motion is released to discover the relationship between external wave and inner tank sloshing. To avoid the box move along with wave, a spring was considered. The results were compared with existing experimental results, and sloshing force and moment were included.

1 INTRODUCTION

With the increasing demands for natural gas and sources in deep sea, ships with partially filled tanks become more and more popular. With the existence of partially filled tanks, the performance of ship motion is different from that without tanks. The ship motion is an external excitation for sloshing tanks, and sloshing tanks would influence ship motion in return. Therefore, the study for the fully coupled effects on ship motion and sloshing tank is necessary.

Many studies have been done between ship motion and sloshing tanks. Rognebakke and Faltinsen [1] conducted two-dimensional experiments about hull section with two tanks in waves. Zhao et al [2] conducted model test of a 2-D FLNG section with sloshing tanks, and then applied time-domain method to study the coupling effect between ship motion and sloshing tanks. Nasar et al [3] carried out a 3-D experiments of rectangular tanks with a barge in waves. Lee et al [4] applied a newly developed Moving Particle Semi-implicit (MPS) method to study the 2-D coupling effects of sloshing tank and ship motion. With the development of computer science, the implement of computational fluid dynamics (CFD) becomes essential for numerical simulation. Some researchers applied CFD methods on sloshing tanks to capture the violent flow. Lee et al [5] applied potential-viscous hybrid method to simulate the coupling effects between ship motion and sloshing tanks; Jiang et al [6], Li et al [7] both applied CFD methods to simulate the inner sloshing tanks, and potential theory to simulate the ship motion. Our group have discussed fully coupled effects between ship motion and sloshing tanks both in CFD methods [8][9][10]. However, the coupling effects discussed before were under wave conditions, the ship motion was coupled in two or more degrees of freedom, the coupling effects have not been studied deep enough.

In this paper, fully coupled effects on ship motion with a single sloshing tank is discussed using our in-house CFD solver naoe-FOAM-SJTU, which is developed and based on open source toolbox OpenFOAM. This paper simulates a box-shaped hull with a partially filled single tank. Two different wave conditions are considered, and sloshing forces are included. In order to calculate the inner sloshing force, the function of calculating forces and moments on patches are added, and constant damp force is included. The details of inner sloshing and external exciting wave are also discussed.

2 NUMERICAL METHOD

2.1 Governing Equation

The incompressible Reynolds-Averaged Navier-Stocks equations are adopted in this paper to investigate the viscous flow. Using dynamic deformation mesh, the governing equations are:

$$\nabla \bullet \mathbf{U} = 0 \tag{1}$$

$$\frac{\partial \rho \mathbf{U}}{\partial t} + \nabla \bullet (\rho(\mathbf{U} - \mathbf{U}_g)\mathbf{U}) = -\nabla p_d - \mathbf{g} \bullet \mathbf{x} \nabla \rho + \nabla \bullet (\mu_{eff} \nabla \mathbf{U}) + (\nabla \mathbf{U}) \bullet \nabla \mu_{eff} + f_\sigma + f_s \tag{2}$$

Where $\mathbf{U}$ is velocity field, $\mathbf{U}_g$ is velocity of grid nodes; $p_d = p - \rho \mathbf{g} \bullet \mathbf{x}$ is dynamic pressure; $\mu_{eff} = \rho(\nu + \nu_t)$ is effective dynamic viscosity, in which ν and ν_t are kinematic viscosity and eddy viscosity respectively. ν_t is obtained by *k-ω* SST turbulence model[11]. f_σ is the surface tension term in two phases model.

The solution of momentum and continuity equations is implemented by using the pressure-implicit spit operator (PISO) algorithm [12]. PISO algorithm applies mass conservation into pressure equation, thus when pressure equation converges, continuity error decreases. This method uses a predictor-corrector on solving pressure-velocity coupling, and utilizes a collocated grid method [13].

2.2 VOF Method

The Volume of fluid (VOF) method with bounded compression techniques is applied to control numerical diffusion and capture the two-phase interface efficiently. The VOF transport equation is described below:

$$\frac{\partial \alpha}{\partial t} + \nabla \bullet [(\mathbf{U} - \mathbf{U}_g)\alpha] = 0 \tag{3}$$

Where α is volume of fraction, indicating the relative proportion of fluid in each cell and its value is always between zero and one:

$$\begin{cases} \alpha = 0 & \text{air} \\ \alpha = 1 & \text{water} \\ 0 < \alpha < 1 & \text{interface} \end{cases} \tag{4}$$

2.3 6DOF Motions

A fully 6DOF module with bodies is implemented. Two coordinate systems are used to solve 6DOF equation. We describe $(x_1, x_2) = (x, y, z, \varphi, \theta, \psi)$ as the translation and rotation angles of the ship, representing motions of surge, sway, heave, roll, pitch and yaw, respectively. $(v_1, v_2) = (u, v, w, p, q, r)$ are the velocities in the earth-fixed coordinate system, which can be transformed to the body-fixed coordinate system by equations given below:

$$v_1 = J_1^{-1} \cdot \dot{x}_1 \quad v_2 = J_2^{-1} \cdot \dot{x}_2 \tag{5}$$

where J_1, J_2 are transformation matrices based on Euler angle. The forces and moments are projected into the earth-fixed system in following way:

$$F=(X,Y,Z)=J_1^{-1}\cdot F_e \quad M=(K,M,N)=J_1^{-1}\cdot M_e \tag{6}$$

2.4 Patch forces and moments

In order to compute the sloshing forces and moments, the single body is divided into several patches. In present study, the single body is divided into two patches: the hull of box-shaped ship which can reveal external forces and moments, the inner tank which can reveal inner sloshing forces and moments. The forces are integrated on each patch separately, and accumulated as a whole to compute for next motion. The process is shown in Fig.1.

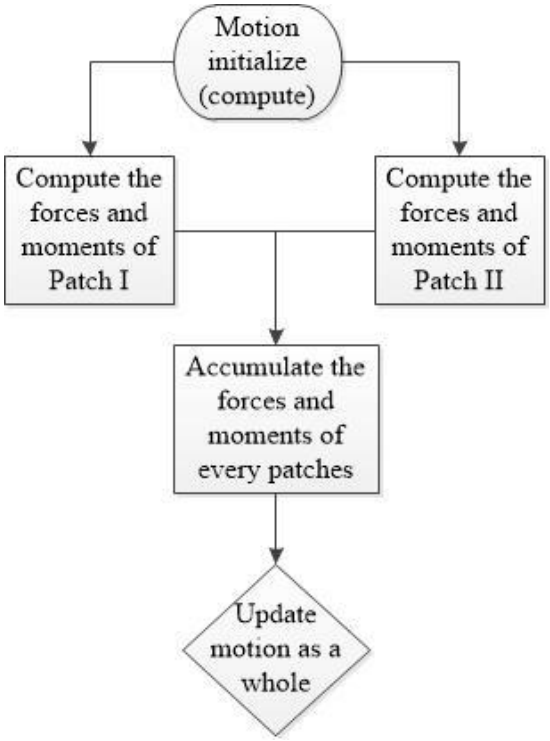

Figure 1: The process of calculating the forces and moments of each patch

2.5 Wave Generation and Damping

The incoming regular wave is generated by imposing the boundary conditions of α and **U** at the inlet. The linear Stokes wave in deep water is applied for the wave generation.

$$\xi(x,t)=a\cos(kx-\omega_e t) \tag{7}$$

$$u(x,y,z,t)=a\omega e^{kz}\cos(kx-\omega_e t) \tag{8}$$

$$w(x,y,z,t)=a\omega e^{kz}\sin(kx-\omega_e t) \tag{9}$$

where ξ is the wave elevation; a is the wave amplitude; k is the wave number; U_0 is the ship velocity; ω is the natural frequency of wave; ω_e is the encounter frequency, in this condition, $\omega_e=\omega$.

3 NUMERICAL RESULTS

3.1 Geometry and Mesh Generation

In order to verify the accuracy of our CFD solver, and discover the coupling effect, a box with two tanks in waves was considered. According to the experiments carried out by Fognebakke and Faltisen[1], the physical model was chosen to be a box-shaped hull section. The details of the hull and tanks are illustrated in

Fig.2 (a), which comes from Fognebakke and Faltisen[1]. The physical model of numerical simulation is shown in Fig.3. In order to obtain the external exciting forces and inner sloshing forces, the model was built in two patches.

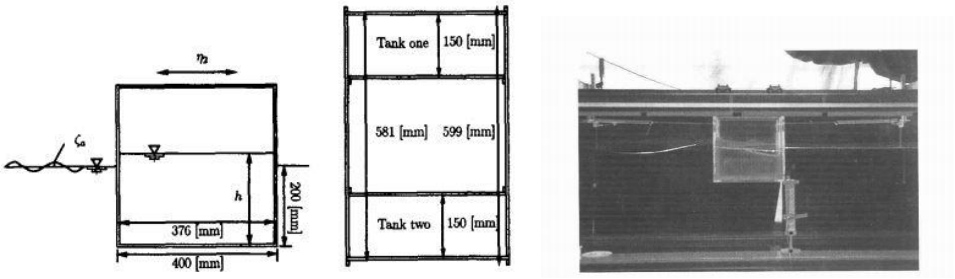

(a) Details of hull section, side and top view (b) Experimental setup

Figure 2: Details of box-shaped hull section and experimental setup. [1]

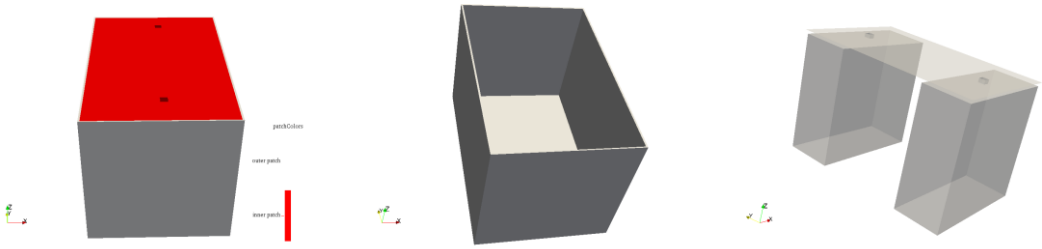

(a) Physical model with different patches (b) Hull (c) Tanks

Figure 3: Physical model with outer patch (hull) and inner patch (tanks)

Fig.4 illustrates the mesh generation of computational domain and the model. The meshes are generated by snappyHexMesh, an auto mesh generation utility provided by OpenFOAM. The total cell numbers are around 1.9 M, and the single tank requires 0.1M cells. For we only simulate one single tank, therefore the grids of other tank which has no fluid in it are not refined. To capture the wave, grids near free surface are required to be refined. Fig.4 (b) shows two small tunnels connected the LNG tanks to the external region, which can keep pressure inside the tanks the same to the external region and simplify the computations. Meanwhile, the connected tunnel makes the computation fully coupled.

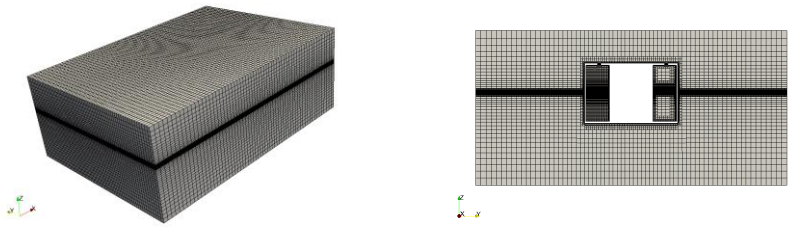

(a) Mesh of computational domain (b) Hull

Figure 4: Demonstrations of meshes

The filling condition of the tank and computational domain setup is shown in Fig.5. Two different wave conditions are chosen in present work, therefore, two computational domains are carried out. The computational domain of large wave length is set as -1.2m<x<1.6m, -1m<y<1m, -0.6m<z<0.4m. The sponge layer is included to avoid the wave reflection and keep mass conservation in computational domain. The hull is allowed to move in sway only, and according to experimental setup, shown in Fig.2 (b), there is a bearing

providing a constant force of 2.0N which acts against the motion. Therefore, we added a constant damp into the hull motion. The hull is excited by regular waves, the simulation conditions are shown in Table 1. In order to prevent the model from drifting off, a spring is included, with total stiffness 30.9N/m.

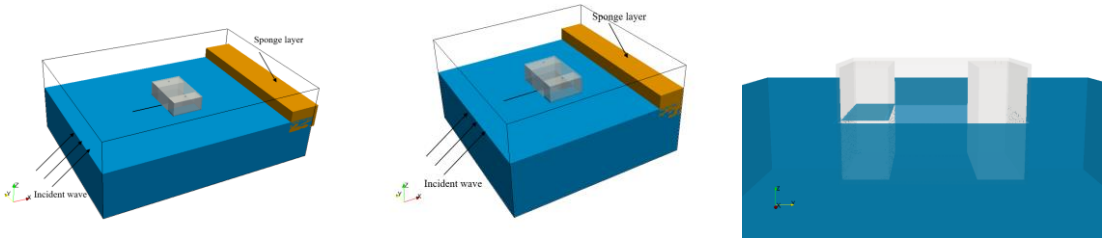

(a) Case of large wave length (b) Case of small wave length (c) Filling condition

Figure 5: Computational domain and filling condition

Table 1: Computational conditions

Case	No. of tanks filled	Filling height (m)	Structural mass (kg)	Wave height (m)	Wave frequency (rad/s)
1	One	0.186m	37.01	0.03	8.6
2					10.8

3.2 Numerical Verification

The time history of sway motion of hull is shown in Fig. 6. The hull would drift away with wave without spring, thus the hull motion shows two states: transient state and steady state. The duration of transient state in case 1 is longer than that in case 2, for the large wave length provide more energy than that of small wave length. To compare with the experimental data, the sway amplitudes from steady state are chosen, illustrated in Table 2. It can be seen from Table 2 that the results of our current work agree well with the experimental results, which proves our current algorithm is reliable.

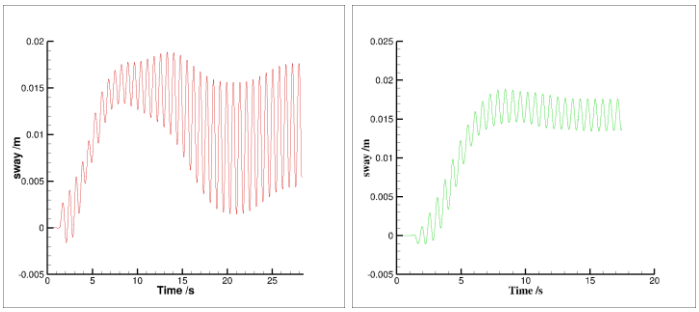

(a) Sway motion in case 1. (b) Sway motion in case 2.

Figure 6: Time history of sway motion of hull

Table 2: Comparison of experimental data and present work in sway motion

Case	Experiment	Present work	Error
1	0.45	0.43	4.4%
2	0.16	0.143	10.6%

3.3 Sloshing Forces and Internal Flow

In order to figure out the influence of sloshing fluid on hull motion, the sloshing forces and the details of internal fluid was discussed. Fig. 7 presents the comparison between sloshing force and external exciting forces in steady state. It can be seen that the exciting forces have phase difference with the internal force in case 1, while have the same phase in case 2. And when during the steady state, the sloshing forces effects the excitation force, for curve of the excitation forces is not sinusoidal. The force of mooring system is also considered, and in both cases, the phase of mooring forces is the same with sloshing force. The mooring system is a spring, thus the magnitude of mooring force is reduced when the hull moves along with the mooring line. That means the sloshing fluid move against the hull motion. It can be observed that in case 1, the value of sloshing force is larger than excitation force, for the exciting wave frequency is near the natural frequency of the liquid in tank, the violent sloshing provides strong sloshing force.

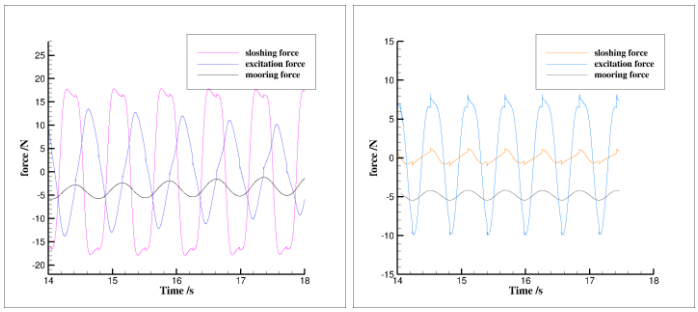

(a) Forces in case 1. (b) Forces in case 2.

Figure 7: Time history of the horizontal sloshing force, excitation force and force of mooring line

The details of inner sloshing and outer fluid are also included. Fig. 8 shows the snapshots of inside and outside fluid motion in case 1, while Fig. 9 shows the snapshots in case 2. In Fig. 8 and Fig.9, snapshots show the instantaneous position of the free surface. It appears that in both cases, there exists phase difference between the internal and external fluid motion. Due to the large motion and resonance between incident wave and liquid in tank, the liquid motion in tank of case 1 is violent. The fluid in tank climbs on the bulkhead and rolls over when the fluid reaches the peak. The details of motion of liquid is illustrated in Fig.10 (a). Divided in the middle of the tank, the fluid flows apart from the boundary line and forms two vortex on the bottom of the tank. The fluid near wave ward side goes up to the peak and then rolls over and goes down. Some of the fluid which turns over and rolls down flows on the surface of the slope, and others rolls into the peak of the fluid, and then flows down along the wave ward bulkhead. These roll over fluid once goes down to the bottom of the tank, the energy makes them to go up again far away from the bulkhead. Then there forms two vortex on the bottom corner.

For case 2, the energy from the wave is small and no resonance happens in tank fluid, thus the sloshing in tank is not violent. Therefore, the details of inner flow in Fig 10 (b) show no vortex. The fluid near wave ward side goes up to climb the bulkhead, while the fluid near lee side goes down. The velocity of the internal fluid on top is larger than that on the bottom, thus when it begins to slosh, the top side moves fast, while the bottom of the fluid moves slow. And for the part of bulkhead, the fluid doesn't flow with the surface part of the inner fluid due to the viscous effects, therefore the fluid in the corner of the bottom shows different forms during sloshing.

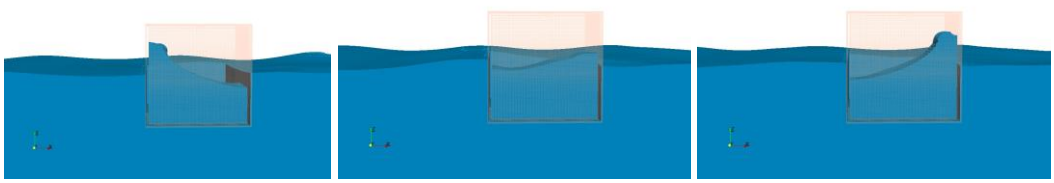

Figure 8: Snapshots of motion fluid inside and outside in case 1.

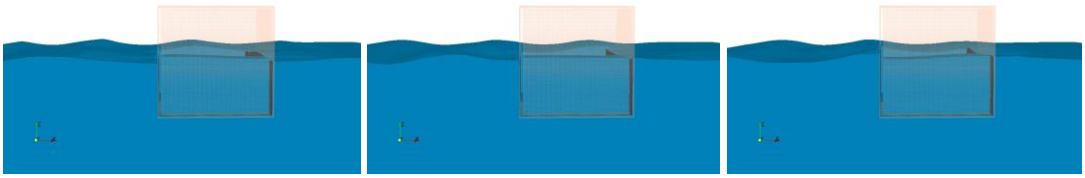

Figure 9: Snapshots of motion fluid inside and outside in case 2.

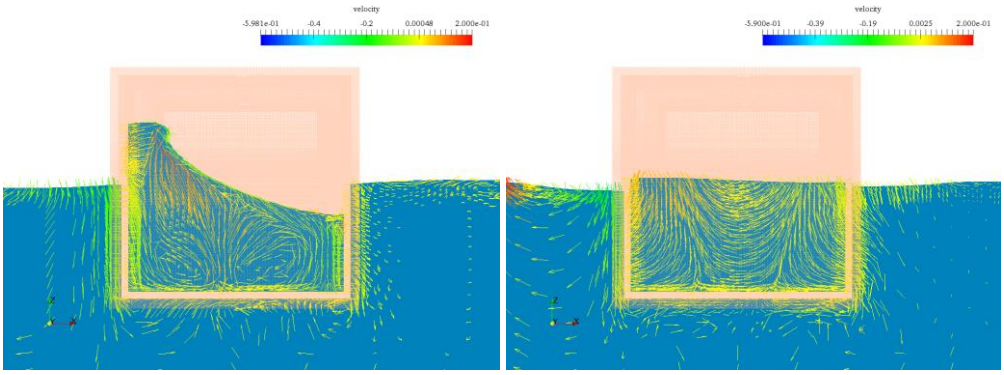

(a) Vector of velocity in tank in case 1. (b) Vector of velocity in tank in case 2.

Figure 10: Vector of velocity of liquid in tanks.

4 CONCLUSION

In this paper, the coupling effects are discussed using our in house solver naoe-FOAM-SJTU. The box-shaped hull is equipped with two tanks, with only one tank partially filled. Only sway motion is considered. The sway motion in two different wave frequencies are compared with experimental results, and shows well agreement, which reveals our solver had the ability to solve the inner fluid sloshing and external fluid simultaneously.

Our in house CFD solver naoe-FOAM-SJTU has added new functions to calculate the internal sloshing forces acting on tank. The model is departed into inner and outer parts to obtain the sloshing forces and external exciting forces. The results are analysed to figure out how the sloshing forces and excitation forces counteract each other. The sloshing forces in tanks have phase differences with external exciting forces when the wave frequency equals to 8.6 rad/s, while when the wave frequency equals to 10.8 rad/s, there exists no phase differences between sloshing forces and excitation forces. Besides, for the thickness of the bulkhead is small, the sloshing force influences the excitation forces to some extent.

At last, the sloshing flow and velocity are included to observe the details of sloshing flow. For the wave frequency equals to 8.6 rad/s, close to natural period of inner fluid, the sloshing in tank is violent, shows roll over on the peak of the fluid and forms two vortex on the bottom corner of the tank; while for the wave frequency equals to 10.8 rad/s, the sloshing in tank is almost linear, and no vortex are observed in the tank.

In the future, more wave frequencies and zero filling tank condition will be considered to find out the coupling effects between internal fluid and external fluid.

ACKNOWLEDGEMENTS

This work is supported by the National Natural Science Foundation of China (51379125, 51490675, 11432009, 51579145), Chang Jiang Scholars Program (T2014099), Shanghai Excellent Academic Leaders Program (17XD1402300), Program for Professor of Special Appointment (Eastern Scholar) at Shanghai

Institutions of Higher Learning (2013022), Innovative Special Project of Numerical Tank of Ministry of Industry and Information Technology of China (2016-23/09) and Lloyd's Register Foundation for doctoral student, to which the authors are most grateful.

REFERENCES

1. Rognebakke, O. F.and Faltinsen, O. M. (2003) Coupling of sloshing and ship motions. *Journal of Ship Research* 47, 208-221.
2. Zhao W.H, Yang J.M, Hu Z.Q, et al. (2014) Coupled analysis of nonlinear sloshing and ship motions. *Applied Ocean Research*, 47, 85-97.
3. Nasar, T., Sannasiraj, S. A. and Sundar. V. (2010) Motion responses of barge carrying liquid tank. *Ocean Engineering* , 37, 935-946.
4. Lee, B. H. Park, J. C. and Kim, M. H. (2010) Two-dimensional vessel-motion/liquid-sloshing interactions and impact loads by using a particle method. *Proceedings of the ASME 29th International Conference on Ocean, Offshore and Arctic Engineering*, Shanghai, China.
5. Lee, S. J. and Kim, M. H. (2010) The effects of inner-liquid motion on LNG vessel responses. *Journal of Offshore Mechanics and Arctic Engineering*, 132, 021101.
6. Jiang, S. C., Teng, B., Bai W.and Guo, Y. (2015) Numerical simulation of coupling effect between ship motion and liquid sloshing under wave action. *Ocean Engineering*, 108, 140-154.
7. Li, Y. L., Zhu, R. C., Miao, G. P. and Fan, J. (2012) Simulation of tank sloshing based on OpenFOAM and coupling with ship motions in time domain. *Journal of Hydrodynamics, Ser. B*, 24, 450-457.
8. Shen, Z. R. and Wan, D. C. (2012) Numerical Simulations of Large-Amplitude Motions of KVLCC2 with Tank Liquid Sloshing in Waves. *In Proceedings 2nd Int Conf Violent Flows.* Ecole Centrale Nantes, Nantes, France.
9. Zhuang, Y. and Wan, D. C. (2016) Numerical Study on Coupling Effects of FPSO Ship Motion and LNG Tank Sloshing in Low-Filling Conditions. *Applied Mathematics & Mechanics*, 37, 1378-1393.
10. Yin, C. H., Zhuang, Y. and Wan, D.C.(2016) Numerical Study on Liquid Sloshing in LNG Tanks Coupled with Ship Motion in Waves. *Proceedings of 3rd International Conference on Violent Flows*, 9-11, March 2016, Osaka, Japan, Paper No. 26
11. Issa, R. I. (1986). Solution of the implicitly discretized fluid flow equations by operator-splitting. *Journal of computational physics*, 62, 40-65.
12. Rhie, C. M. and Chow, W. L. (1983). Numerical study of the turbulent flow past an airfoil with trailing edge separation. *AIAA journal*, 21, 1525-1532.
13. Dhakal, T. P. and Walters, D. K. (2009, January). Curvature and rotation sensitive variants of the K-Omega SST turbulence model, *In ASME 2009 Fluids Engineering Division Summer Meeting*. American Society of Mechanical Engineers. 2221-2229.